

Surface and subsurface alterations induced by deep rolling of hardened AISI 1060 steel

A. M. Abrão · B. Denkena · B. Breidenstein · T. Mörke

Received: 8 January 2014 / Accepted: 19 March 2014 / Published online: 27 March 2014
© German Academic Society for Production Engineering (WGP) 2014

Abstract Among the several processes available for the inducement of compressive residual stresses by means of cold work hardening, deep rolling is one of the most widely used especially in the case of solid rotationally symmetrical components, such as axles and shafts. This work investigates the effect of two deep rolling parameters, namely rolling pressure and number of passes, on the surface topography, surface near residual stress, amount of retained austenite and subsurface microhardness distribution of hardened AISI 1060 steel. The results show that after deep rolling the surface topography is characterized by a plasticized zone without evidence of spalling or cracks. A 10-fold decrease in surface roughness is provided by deep rolling and an appreciable reduction was observed for the material ratio curve parameters. Compressive residual stresses were found near the surface after deep rolling and increased particularly with an increase in rolling pressure. In contrast, the highest value for the full width at half maximum was recorded under the lightest deep rolling condition. The amount of retained austenite reached its highest value when rolling with pressure of 200 bar and one pass and was associated with the thickness of the white layer. Finally, the microhardness beneath the surface increased with rolling pressure and was negatively affected by number of passes.

Keywords Deep rolling · Hardened steel · Surface roughness · Residual stress · White layer · Microhardness

1 Introduction

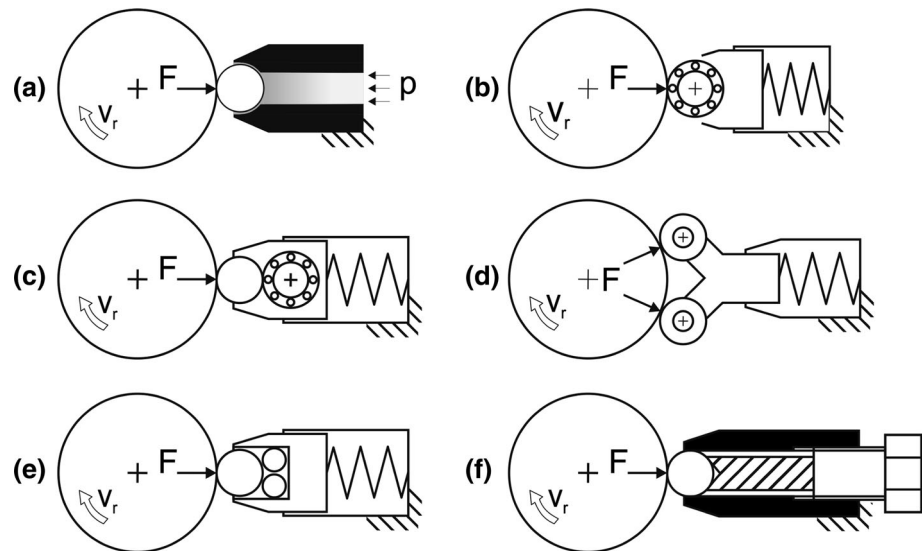
Deep rolling, deep cold rolling, ball or roller burnishing, low plasticity burnishing or simply burnishing are terms indistinctly used by different authors to refer to the same group of operations aimed at the inducement of compressive residual stresses on the surface layers of the processed component. The former will be used in the present work mainly for the sake of consistency and secondly due to the fact that burnishing may eventually suggest that relative movement between tool and workpiece takes place (and consequently friction), which is the case for a rather limited number of publications. An account on the development of cold working is provided by Bush et al. [1], who stated that despite the fact that the first record of rolling occurred in France in 1553, its beneficial influence on mechanical properties was reported for the first time more than three centuries later.

In order to steadily hold the tool against the workpiece under a predetermined load, a number of apparatus are reported in the published literature and a selection of these devices is presented in Fig. 1. The use of hydrostatic pressure to force the rolling tool against the workpiece (Fig. 1a) is probably the most popular method and, in addition to the fact that it is commercially available, other advantages are the reduced number of contact elements (wear and losses are minimized) and the fact that the hydraulic fluid can be used as lubricant. A second group relies on the elastic force in order to apply the required load on the work surface (Fig. 1b, e) and prototypes built using this principle are depicted in [2–5]. Finally, a third category

A. M. Abrão (✉)
Universidade Federal de Minas Gerais, Av. Antônio Carlos 6627
Pampulha, Belo Horizonte, MG 30270-901, Brazil
e-mail: abrao@ufmg.br

B. Denkena · B. Breidenstein · T. Mörke
Institute of Production Engineering and Machine Tools, Leibniz
Universität Hannover, An der Universität 2, 30823 Garbsen,
Germany

Fig. 1 Selection of deep rolling devices based on the working principle: **a** hydrostatic pressure, **b** spring and bearing [2], **c** spring, bearing and roller [3], **d** spring and two bearings [4], **e** spring and three balls [5] and **f** bolt and ball [6]



Ab/73816 © IFW

of deep rolling devices depends on the force directly exerted by the tool against the component (usually applied by means of bolts), as represented in Fig. 1f, [6]. Tailor-made equipment possesses the advantage of being designed and built for a specific purpose and range of operation, however, a major concern is the occurrence of vibration and its deleterious consequences when higher rolling loads are applied. An alternative approach is given by Maximov et al. [7], who proposed a toroidal shaped deep rolling tool that ensures continuous contact between tool and workpiece. Nevertheless, in this case each workpiece diameter requires a specific tool and it is not possible to deep roll surfaces with variable profile or diameter. Apparatus designed to simultaneously cut and deep roll [8–10] and the use of vibration or ultrasonically assisted deep rolling [11, 12] are also proposed in order to, respectively, reduce manufacturing time and improve the process performance.

The analytical approach on deep rolling takes into account only the elastic contact between two curved surfaces (with the possibility of one of them having infinite radius), therefore, in order to consider plastic deformation and thus estimate the induced residual stresses, numerical models must be employed. Sartkulvanich et al. [13] compared experimental and numerical data regarding deep rolling of hardened bearing steel (58–60 HRC) and found that the surface roughness increased with rolling feed rate, however, experimental and numerical results were discrepant probably due to the simplifying assumptions employed in the latter. Better agreement was obtained for the residual stresses distribution, with both experimental and numerical results indicating that compressive stresses of higher intensity were generated using lower rolling feed and higher pressure. Finally, the authors asserted that the residual stresses introduced by previous hard turning were

not relevant for the simulation of the residual stress state after deep rolling.

Despite the fact that the principal goal of deep rolling is the inducement of compressive residual stresses, its effect on the surface quality of the component cannot be neglected, especially in cases where hard turning poses as an alternative to grinding. Under these circumstances, the combination of hard turning followed by deep rolling may result in surface features comparable to grinding at considerably higher production rates. The surface finish of hard turned low alloy steel (59–61 HRC) subjected to super finishing and deep rolling was investigated by Grzesik and Żak [3], who reported that super finishing produced surfaces with superior quality, followed by deep rolling associated with previous hard turning with tools possessing standard geometry (in comparison with wiper geometry).

As far as the influence of deep rolling parameters on the material ratio curve (also known as bearing area curve or Abbott-Firestone curve) is concerned, Tekkaya et al. [14] compared the reduced peak height (Rpk) and reduced valley depth (Rvk) of tungsten carbide sprayed surfaces subjected to deep rolling and grinding and noted that similar Rpk values were generated by both processes, whereas considerably lower Rvk was obtained after grinding. While a low Rvk may represent a reduction in the friction coefficient, the opposite means higher capacity for lubricant retention. When deep rolling, the slope of the material ratio curve increases with rolling feed [11], which is an undesirable effect. Świrad [15] studied three dimensional roughness parameters after deep rolling a low alloy steel using polycrystalline diamond roller tools and noticed that, in general, the amplitude and functional (core roughness depth Sk and reduced peak height Spk) parameters tend to decrease after this operation.

Bouزيد et al. [16] investigated the influence of deep rolling on the surface quality and residual stress of a medium carbon steel subjected to either turning or grinding and found that the roughness resulting from the previous machining operation affected the performance of deep rolling, i.e., under the same deep rolling conditions lower surface roughness was obtained for the ground samples. With regard to the residual stresses, the tensile axial stresses and the neutral perpendicular stresses generated by both grinding and turning changed to compressive stresses after deep rolling.

The hardness profile beneath the surface of a hardened cold work die steel was assessed by Brinksmeier et al. [17], who noticed that its value increased with applied force, nevertheless, its influence on the depth of the affected zone was minimal. Moreover, the amount of retained austenite decreased after deep rolling (as the result of martensite transformation) and contributed, together with strain hardening, to the elevation of the hardness. Similar results were reported by Morimoto [18], who added that the extent of surface work hardening decreased as the number of passes was elevated and that deep rolling employing two or three passes resulted in approximate and considerably higher microhardness values beneath the surface in comparison with a single pass.

Despite the efforts put on the investigation of deep rolling over the last decades, a number of aspects has not been fully elucidated so far. For instance, the relationship between work material properties and deep rolling parameters deserves further attention and may be the reason why inconsistent results are frequently observed. Therefore, the goal of the present work is to investigate the influence of deep rolling pressure and number of passes on the surface and subsurface alterations induced on hardened AISI 1060 hardened steel, thus contributing to the better understanding of the involved phenomena.

2 Experimental procedure

Figure 2 shows the experimental procedure schematically. AISI 1060 high carbon steel was used to produce the specimens for rotating bending fatigue tests in accordance with DIN 50113 standard [19]. The samples were initially rough turned with an oversize of 2 mm in diameter and then subjected to quenching and tempering to reach an average hardness of 756 HV_{0.5}. Finish turning to attain the final diameter of 7 mm was undertaken without cutting fluid in a high stiffness Gildemeister CNC lathe model CTX 520 linear at a cutting speed of 100 m/min, feed rate of 0.1 mm/rot and maximum depth of cut of 0.15 mm using ISO grade P15 coated tungsten carbide inserts (Sandvik Coromant DNMG 110408-PM 4215) mounted on

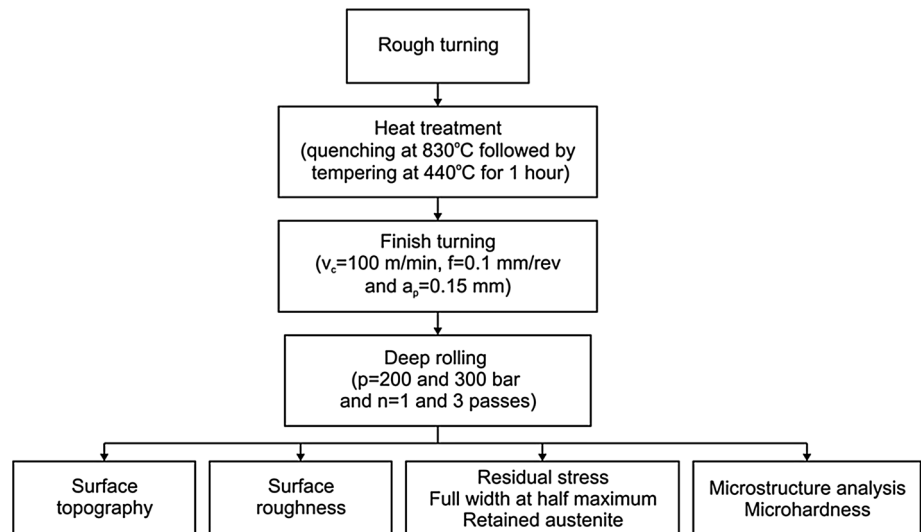
a tool holder coded DDNNN 2020 K11. For deep rolling, an Ecoroll device model HG6-20-5.5-SL20 was attached to the same machine tool and connected to a hydraulic unit (maximum pressure of 400 bar and fluid viscosity of 46 mm²/s at 40 °C), as indicated in Fig. 3. This device operates with three equally spaced tungsten carbide balls (Ø 6.35 mm) in order to avoid the deflection of slender components. The range of the tested deep rolling parameters is as follows: rolling pressures (p) of 200 and 300 bar, one and three rolling passes ($n = 1$ and $n = 3$), constant rolling speed (v_r) of 100 m/min and constant rolling feed (f_r) of 0.07 mm/rot. The tested values for rolling pressure were selected based on the fact that the yield strength of the work material must be exceeded in order to promote plastic deformation and work hardening of the surface layers and that the maximum pressure provided by the hydraulic pump. In the present case, the average yield strength of the hardened AISI 1060 steel is $R_{p0.2} = 1,606$ MPa.

The surface topography of the specimens was assessed with a Zeiss EVO 60 scanning electron microscope and the data concerned with the roughness and material ratio curve parameters were collected using a Mahr Perthometer PGK (sampling length of 0.80 mm). The values of the axial residual stress, full width at half maximum and the volume fraction of retained austenite were obtained with a GE XRD 3003 TT X-ray diffractometer. The $\sin^2\Psi$ method was employed using $\text{CrK}\alpha$ radiation on 211 planes of the ferrite phase and with Ψ varying from -45° to 45° . Finally, the profile of the microhardness distribution beneath the surface was measured with a Struers Duramin-5 hardness tester employing a load of 100 g during 10 s after grinding (SiC paper with 220, 500 and 1,200 mesh sizes) and polishing (3 and 1 μm diamond suspension) the cross sections of the samples.

3 Results and discussion

The surface topographies obtained after turning as well as mild (lowest rolling pressure and least number of passes, i.e., $p = 200$ bar and $n = 1$) and severe (highest rolling pressure and largest number of passes, i.e., $p = 300$ bar and $n = 3$) deep rolling are presented in Fig. 4. It can be seen that the feed marks left by the turning tool (Fig. 4a) are flattened after deep rolling at the lowest pressure and least number of passes ($p = 200$ bar and $n = 1$, respectively) as the result of exceeding the yield point of the material (Fig. 4b). However, applying the highest pressure ($p = 300$ bar) along three rolling passes, see Fig. 4c, did not result in any remarkable further improvement on the surface quality. In contrast to previous reports [4, 11], deep rolling induced defects such as spalling due to overhardening and cracks were not found. Figure 4d compares the roughness profiles obtained after turning (black line) and deep rolling at $p = 200$ bar and

Fig. 2 Schematics of the experimental work



Ab/75640 © IFW

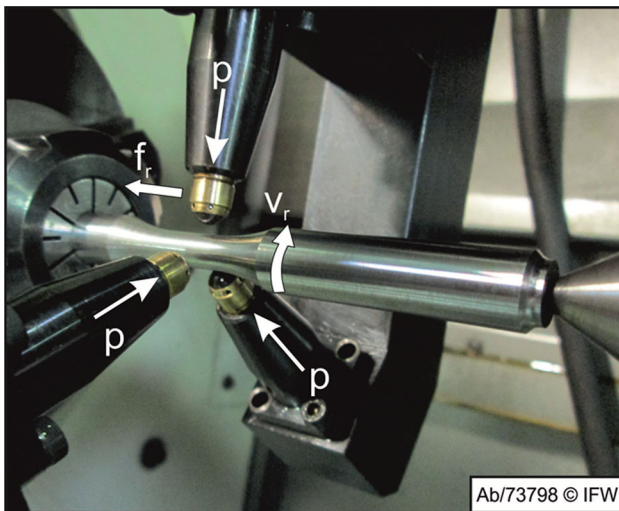


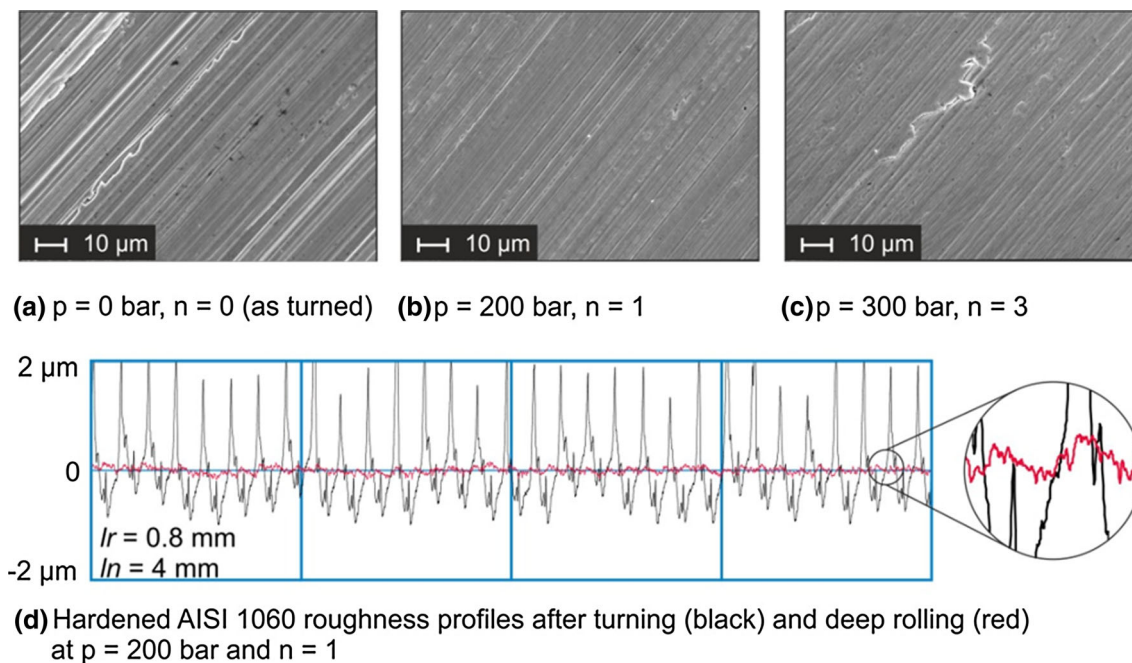
Fig. 3 Deep rolling of hardened AISI 1060 steel

$n = 1$ (red line) and shows a substantial reduction in the height of the peaks and depth of valleys owing to plasticization. Finally, a detail of the surface profile after deep rolling shows the rolling feed marks. Together with the expected inducement of compressive residual stresses, the roughness profile generated by deep rolling can significantly improve the component fatigue life by means of the minimization of regions more prone to crack initiation.

Figure 5 shows the average surface roughness of hardened AISI 1060 steel after turning and deep rolling based on the arithmetic average height (Ra) and maximum peak to valley height in the assessment length (Rt). The values obtained for the turned samples ($Ra = 0.61 \mu\text{m}$ and $Rt = 4.82 \mu\text{m}$) decrease by one order of magnitude after deep rolling at the mildest condition, i.e., $p = 200$ bar and $n = 1$ to reach $Ra = 0.05 \mu\text{m}$ and $Rt = 0.47 \mu\text{m}$,

nevertheless, the additional elevation of rolling pressure and/or number of passes does not represent any appreciable further reduction in Rt (as can be inferred by the scatter lines), while slightly lower Ra values are obtained under the highest pressure (average of $0.04 \mu\text{m}$ with standard deviation of 0.01). This behaviour can be explained by the fact that as the yield point of the work material is exceeded, plastic flow takes place irrespectively of the elevation in pressure or number of passes. As a matter of fact, extreme rolling conditions may lead to excessive bulging or spalling, thus impairing the quality of the surface.

Figure 6a shows a typical material ratio curve resulting from deep rolling with the following functional parameters: Rvk , core roughness depth (Rk), Rpk and the material portions of the highest peaks and deepest valleys ($Mr1$ and $Mr2$, respectively). These data are relevant not only for plateau-honed surfaces but also to components used in bearing or tribological applications. Figure 6b shows the superposed curves obtained under each deep rolling condition, where it can be inferred that the influence of the number of rolling passes is almost imperceptible, i.e., considering constant rolling pressure values (either $p = 200$ bar or $p = 300$ bar), the elevation of number of passes from $n = 1$ (drawn in black) to $n = 3$ (drawn in red for $p = 200$ bar and in green for $p = 300$ bar) does not alter the shape of the material ratio curves. On the other hand, increasing rolling pressure from 200 to 300 bar causes a reduction in the slope of the curves. This effect can be regarded as positive since it represents a reduction of the void volume in the core region. Although the influence of deep rolling on the material portions is not evident in Fig. 6b, both values were slightly reduced, which can also be considered beneficial (especially of $Mr2$ which is also related to the capacity for lubricant retention).



Ab/73818 © IFW

Fig. 4 Effect of deep rolling parameters on the surface topography (a–c), superposing of turned (in black) and deep rolled (in red) roughness profiles with a detail of the deep rolled profile (d)

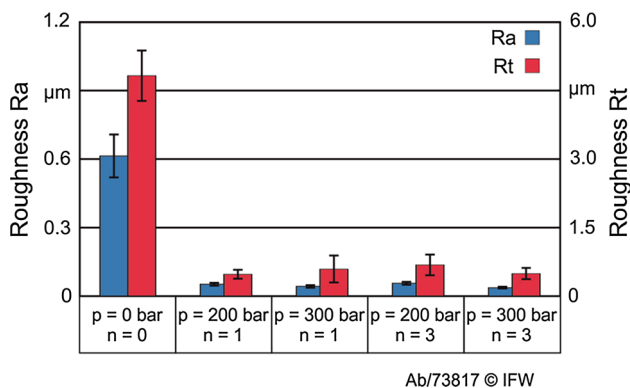


Fig. 5 Effect of rolling pressure and number of passes on amplitude roughness parameters R_a and R_t

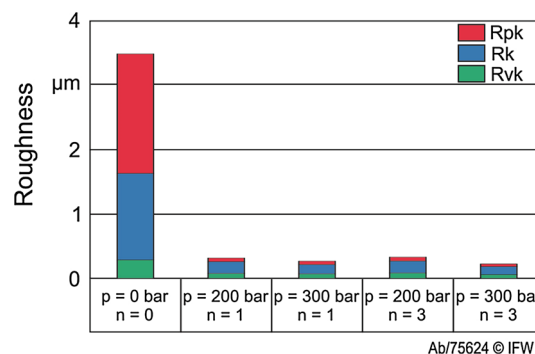


Fig. 7 Effect of rolling pressure and number of passes on the roughness functional parameters R_{vk} , R_k and R_{pk}

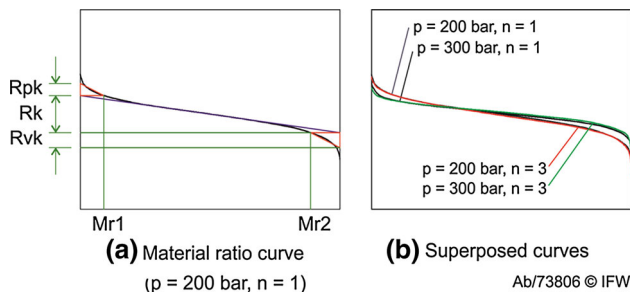


Fig. 6 Typical material ratio curve obtained after deep rolling (a) and superposed material ratio curves (b)

A comparison between the values of R_{vk} , R_k and R_{pk} after turning and deep rolling is presented in Fig. 7. As suggested by Fig. 4d, the distribution of the turned surface is characterized by high R_k and R_{pk} values and low R_{vk} . After deep rolling at $p = 200$ bar and $n = 1$ R_{pk} is drastically reduced to 3 % of its initial value, which represents a positive effect with regard to the wear behaviour of the component (reduction of the portion to be worn away during running-in). Although to a lesser extent, the values of R_k and R_{vk} are also reduced (13 and 28 % of the values given by turning), which can be considered drawbacks due to the fact that R_k is associated with a more uniform wear behaviour and R_{vk} is related to the surface capacity for oil retention and resistance to adhesion.

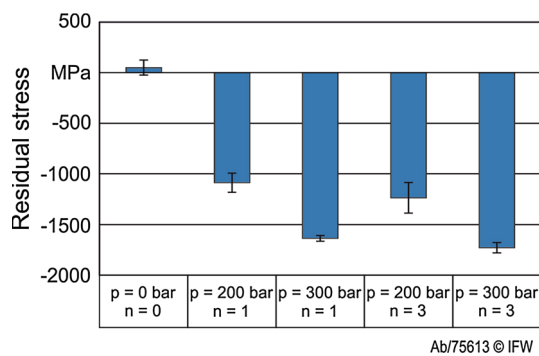


Fig. 8 Effect of rolling pressure and number of passes on the axial residual stress

The influence of the investigated deep rolling parameters on the axial residual stress (stress uniformly distributed on the macroscopic scale) near the surface is presented in Fig. 8, in addition to the average value recorded for the turned samples. It can be noted that the slightly tensile residual stress induced by turning (50 MPa) changes to compressive values after deep rolling. Moreover, the intensity of the compressive stress increases appreciably with rolling pressure and marginally with number of passes to reach a maximum value of $-1,730$ MPa using $p = 300$ bar and $n = 3$. As rolling pressure and number of passes are elevated, more severe work hardening takes place and promotes the elevation of the residual stress near the surface.

Nevertheless, a distinct scenario is observed with regard to the broadening of the diffraction peak (full width at half maximum) measured near the surface and shown in Fig. 9. This parameter gives an indication of the microresidual stress, i.e., the stress resulting from inhomogeneous plastic strain distribution on the microscopic scale. Differently from the results presented in Fig. 8, the broadest width of the diffraction peak is recorded when deep rolling at the mildest condition ($p = 200$ bar and $n = 1$). This behaviour can be explained by the Hertzian nature of the contact between the rolling tool and the workpiece, which results in maximum equivalent stress at a specific depth beneath the surface depending on the applied force and on the radius, Young modulus and Poisson ratio of the tool and workpiece. The higher the pressure and the number of passes, the deeper the position where the maximum equivalent stress is applied [20]. Additionally, Krauss [21] reports that with cold work, a substructure characterized by dislocation walls surrounded by dislocation free cells develops. Increasing cold work these cells decrease in size and the walls become better defined. Therefore, in contrast with the residual stress which increases with the deep rolling parameters, the full width at half maximum stress presents maximum under a specific deep rolling condition.

Figure 10 shows that the volume fraction of retained austenite after deep rolling at $p = 200$ bar and $n = 1$ is

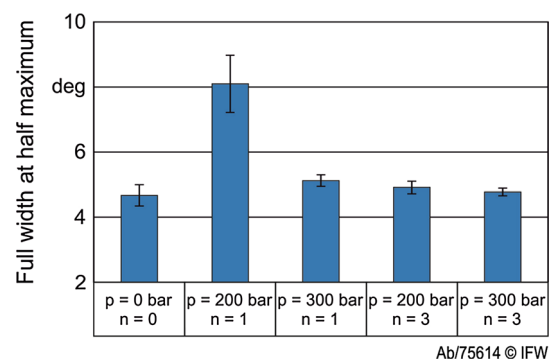


Fig. 9 Effect of rolling pressure and number of passes on the full width at half maximum near the surface

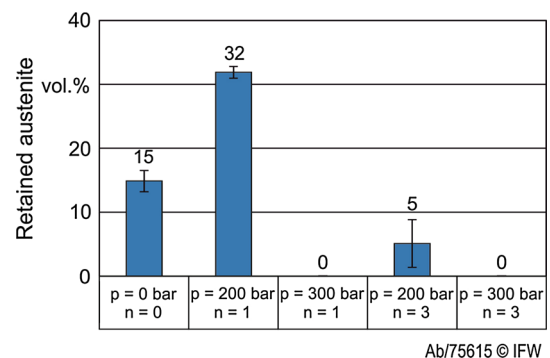
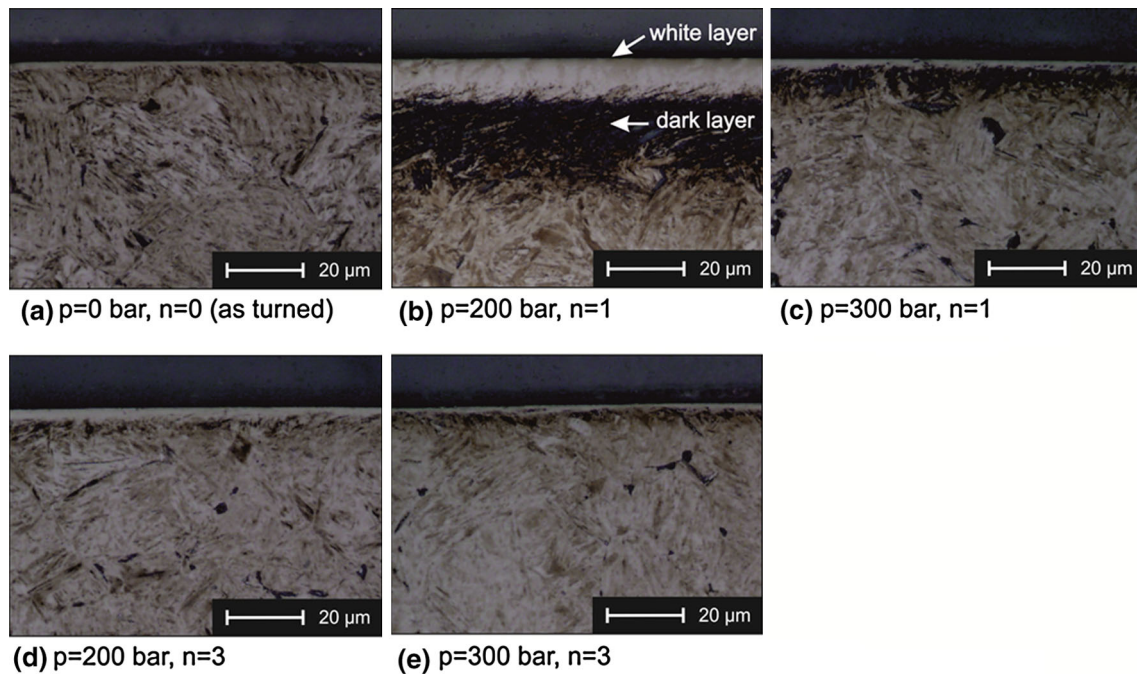


Fig. 10 Effect of rolling pressure and number of passes on the volume fraction of retained austenite near the surface

higher than after turning. Deformation induced phase transformation can be observed during deep rolling of steels containing retained austenite [20], therefore, this result was unexpected owing to the fact that with cold work the amount of retained austenite should decrease. Indeed, the supplementary elevation of pressure and number of passes did promote the reduction of the amount of retained austenite, which was most probably transformed into martensite. These findings can be explained by the micrographs of the etched cross sections of the specimens (Fig. 11). The presence of an external white layer followed by a dark layer is typically observed after machining hardened steels, see Fig. 11a. The former is produced when the austenitization temperature is reached in the machined surface followed by rapid cooling (quenching), while the latter is generated in the region beneath the surface where lower temperatures are achieved followed by cooling at a slower rate (tempering). A review presented by Guo and Sahni [22] reports that the white layer comprises of martensite and austenite, however, a consensus regarding the volume fraction of these structures has not been achieved yet. Figure 11b shows that the thickest white layer is produced after deep rolling at $p = 200$ bar and $n = 1$. Owing to the fact that the X-ray penetration depth ranges from 2.49 to 5.83 μm (as the



Ab/73807 © IFW

Fig. 11 Cross sections of hardened AISI 1060 steel after deep rolling: **a** $p = 0$ bar and $n = 0$, **b** $p = 200$ bar and $n = 1$, **c** $p = 300$ bar and $n = 1$, **d** $p = 200$ bar and $n = 3$ and **e** $p = 300$ bar and $n = 3$

scattering angle varies from 50° to 163°), the detected amount of retained austenite increases with the thickness of the white layer within this range. Moreover, Fig. 11c, e indicate the presence of a white layer slightly thicker than that produced by turning alone. Reports on the development of the white layer under conditions which do not involve the austenitization temperature, such as impact and rolling contact, are available in the published literature. More specifically, the formation of a white layer due to severe plastic deformation of a rail disc is described by Carroll and Beynon [23], however, its inducement by deep rolling is not clear and deserves further investigation.

The profiles of the microhardness distributions beneath the surface are represented in Fig. 12. Owing to the size of the indentations, the measurements started at $45 \mu\text{m}$ from the border, therefore, the hardness of the white layer could not be determined. It can be noticed that the microhardness increased after deep rolling and despite the scatter in the data, it can be inferred that rolling pressure is responsible for the elevation of microhardness, while the elevation of number of passes will cause a decrease in microhardness. While the elevation of rolling pressure represents more work hardening, an increase in the number of passes may lead to a better distribution of dislocations, thus preventing the elevation of microhardness, especially in the present case where three rolling balls act simultaneously. According to [24, 25], the maximum hardness value increases and shifts from the surface with applied pressure,

however, exceeding a certain pressure value there is no additional hardness elevation due to work hardening saturation. The latter authors add that under determined circumstances the surface hardness may assume values inferior to those recorded prior to deep rolling.

4 Conclusions

After deep rolling hardened AISI 1060 high carbon steel ($756 \text{ HV}_{0.5}$) under various conditions the following conclusions can be drawn:

- The surface topography generated by deep rolling is characterized by flattened peaks and valleys filled with material due to plastic flow. Evidences of spalling or cracks were not found within the tested range.
- A 10-fold decrease in surface roughness was obtained after deep rolling at the mildest condition, with Ra decreasing from 0.61 to $0.05 \mu\text{m}$ and Rt from 4.82 to $0.47 \mu\text{m}$. The elevation of rolling pressure and/or number of passes did not represent any appreciable further reduction in these roughness parameters.
- The functional parameters collected from the material ratio curve indicate that compared with the turned specimens, deep rolling positively affected the tribological properties of the material by means of the reduction in the values of Rpk and $Mr2$. As a side effect, the values of Rk and Rvk also decreased.

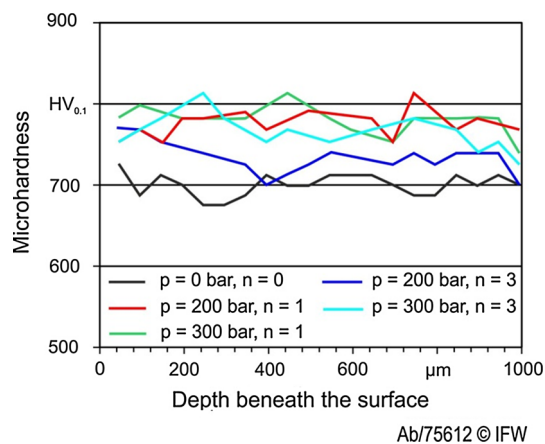


Fig. 12 Effect of rolling pressure and number of passes on the microhardness distribution beneath the surface

- The slightly tensile axial residual stress recorded near the surface after turning changed to compressive stress after deep rolling and increased particularly with rolling pressure to reach $-1,730$ MPa using a pressure of 300 bar and three rolling passes. In contrast, the full width at half maximum reached its peak value under the mildest deep rolling condition (pressure of 200 bar and one single pass).
- The volume fraction of retained austenite reached its maximum employing the mildest deep rolling condition, which was also responsible for the thickest white layer on the workpiece subsurface. As rolling pressure and number of passes were further elevated, the amount of retained austenite decreased, thus suggesting their transformation into martensite induced by plastic deformation.
- The values of microhardness measured beneath the surface are higher after deep rolling in comparison with turning and tend to increase with rolling pressure and to decrease with the elevation of number of passes.

Acknowledgments The authors are grateful to the German Research Foundation for funding the Collaborative Research Centre 653. A.M. Abrão would like to express his gratitude to the CAPES Foundation, Ministry of Education of Brazil, for funding his post-doctoral scholarship (Grant No. 10118128). The authors are also indebted to the Institute of Materials Science of the Leibniz Universität Hannover for the heat treatment and mechanical testing of the specimens and to both Ecoroll AG Werkzeugtechnik (Celle, Germany) and Sandvik Tooling Deutschland GmbH for the provision of deep rolling and cutting tools, respectively.

References

1. Bush GF, Almen JO, Danse LA, Heiss JP (1962) How, when and by whom was mechanical prestressing discovered. In: Soc Automot Eng ISTC, Div. 20 Meeting, SAE, Colorado Springs, Colorado

2. Hamadache H, Laouar L, Zeghib NE, Chaoui K (2006) Characteristics of Rb40 steel superficial layer under ball and roller burnishing. *J Mater Process Technol* 180:130–136
3. Grzesik W, Żak K (2012) Modification of surface finish produced by hard turning using superfinishing and burnishing operations. *J Mater Process Technol* 212:315–322
4. El-Axir MH (2000) An investigation into roller burnishing. *Int J Mach Tools Manuf* 40:1603–1617
5. Hassan AM, Momani AMS (2000) Further improvements in some properties of shot peened components using the burnishing process. *Int J Mach Tools Manuf* 40:1775–1786
6. Loh NH, Tam SC, Miyazawa S (1993) Ball burnishing of tool steel. *Precis Eng* 15(2):100–105
7. Maximov JT, Kuzmanov TV, Duncheva GV, Ganev N (2009) Spherical motion burnishing implemented on lathes. *Int J Mach Tools Manuf* 49:824–831
8. Segawa T, Sasahara H, Tsutsumi M (2004) Development of a new tool to generate compressive residual stress within a machined surface. *Int J Mach Tools Manuf* 44:1215–1221
9. Axinte DA, Gindy N (2004) Turning assisted with deep cold rolling—a cost efficient hybrid process for workpiece surface quality enhancement. *J Eng Manuf* 218:807–811
10. Denkena D, Breidenstein B, de Leon L, Dege J (2010) Development of combined manufacturing technologies for high strength structural components. *Adv Mater Res* 137:219–246
11. Pande SS, Patel SM (1984) Investigations on vibratory burnishing process. *Int J Mach Tools Des Res* 24:195–206
12. Loh NH, Tam SC (1988) Effects of ball burnishing parameters on surface finish—a literature survey and discussion. *Precis Eng* 10(4):215–220
13. Sartkulvanich P, Altan T, Jasso F, Rodriguez C (2007) Finite element modelling of hard roller burnishing: an analysis on the effects of process parameters upon surface finish and residual stresses. *J Manuf Sci Eng* 129:705–716
14. Tekkaya AE, Kleiner M, Biermann D, Hiegemann L, Rausch S, Franzen V, Kwiatkowski L, Kersting P (2013) Friction analysis of thermally sprayed coatings finished by ball burnishing and grinding. *Prod Eng Res Dev* 7:601–610
15. Świrad S (2008) The surface texture analysis after sliding burnishing with cylindrical elements. *Wear* 271:576–581
16. Bouzid W, Tsoumarev O, Sai K (2004) An investigation of surface roughness of burnished AISI 1042 steel. *Int J Adv Manuf Technol* 24:120–125
17. Brinksmeier E, Garbrecht M, Meyer D (2008) Surface hardening by strain induced martensitic transformation. *Prod Eng Res Dev* 2:109–116
18. Morimoto T (1988) Work hardening and tool surface damage in burnishing. *Wear* 127:149–159
19. Deutsches Institut für Normung e.V. (1982) DIN 50113 Testing of metallic materials; rotating bending fatigue test (in German)
20. Schultze V (2006) Modern mechanical surface treatment. Wiley-VCH Verlag GmbH & Co, KGaA, Weinheim
21. Krauss G (1990) Steels: heat treatment and processing principles. ASM International, Materials Park
22. Guo YB, Sahni J (2004) A comparative study of hard turned and cylindrically ground white layers. *Int J Mach Tools Manuf* 44:135–145
23. Carroll RI, Beynon JH (2007) Rolling contact fatigue of white etching layer: part 1 crack morphology. *Wear* 262:1253–1266
24. Klocke F, Bäcker V, Wegner H, Feldhaus B, Baron H-U, Hessler R (2009) Influence of process and geometry parameters on the surface layer state after roller burnishing of IN718. *Prod Eng Res Dev* 3:391–399
25. Berstein G, Fuchsbaue B (1982) Festwalzen und schwingfestigkeit. *Z Werkst* 13:103–109